THE JOURNAL OF COMPARATIVE NEUROLOGY 323:341-358 (1992)

Cytoarchitecture and Neural Afferents of Orbitofrontal Cortex in the Brain of the Monkey

R.J. MORECRAFT, C. GEULA, AND M.-M. MESULAM
Bullard and Denny-Brown Laboratories, Division of Neuroscience and Behavioral Neurology, Harvard Department of Neurology, Beth Israel Hospital, Boston, Massachusetts 02215

ABSTRACT

The orbitofrontal cortex of the monkey can be subdivided into a caudal agranular sector, a transitional dysgranular sector, and an anterior granular sector. The neural input into these sectors was investigated with the help of large horseradish peroxidase injections that covered the different sectors of orbitofrontal cortex. The distribution of retrograde labeling showed that the majority of the cortical projections to orbitofrontal cortex arises from a restricted set of telencephalic sources, which include prefrontal cortex, lateral, and inferomedial temporal cortex, the temporal pole, cingulate gyrus, insula, entorhinal cortex, hippocampus, amygdala, and claustrum. The posterior portion of the orbitofrontal cortex receives additional input from the piriform cortex and the anterolateral portion from gustatory, somatosensory, and premotor areas.

Thalamic projections to the orbitofrontal cortex arise from midline and intralaminar nuclei, from the anteromedial nucleus, the medial dorsal nucleus, and the pulvinar nucleus. Orbitofrontal cortex also receives projections from the hypothalamus, nucleus basalis, ventral tegmental area, the raphe nuclei, the nucleus locus coeruleus, and scattered neurons of the pontomesencephalic tegmentum.

The non-isocortical (agranular-dysgranular) sectors of orbitofrontal cortex receive more intense projections from the non-isocortical sectors of paralimbic areas, the hippocampus, amygdala, and midline thalamic nuclei, whereas the isocortical (granular) sector receives more intense projections from the dorsolateral prefrontal area, the granular insula, granular temporopolar cortex, posterolateral temporal cortex, and from the medial dorsal and pulvinar thalamic nuclei. Retrograde labeling within cingulate, entorhinal, and hippocampal cortices was most pronounced when the injection site extended medially into the dysgranular paraolfactory cortex of the gyrus rectus, an area that can be conceptualized as an orbitofrontal extension of the cingulate complex.

These observations demonstrate that the orbitofrontal cortex has cytoarchitectonically organized projections and that it provides a convergence zone for afferents from heteromodal association and limbic areas. The diverse connections of orbitofrontal cortex are in keeping with the participation of this region in visceral, gustatory, and olfactory functions and with its importance in memory, motivation, and epileptogenesis.

Key words: horseradish peroxidase, paralimbic, cytoarchitectonics, connectivity

A host of neuroanatomical studies, very few of which have specifically focused on orbitofrontal cortex, have shown that this region of the monkey brain is interconnected with the lateral prefrontal cortex, posterior parietal cortex, lateral temporal cortex, lateral premotor cortex, cingulate gyrus, temporal pole, parahippocampal cortices, hippocampus, amygdala, nucleus basalis, hypothalamus, claustrum, insula, neostriatum, thalamus, substantia nigra, and pons (Levin, '36; Mettler, '47a,b; Nauta, '61, '64; Kuypers et al., '65; Johnson et al., '68; Pandya and Kuypers, '69; Pandya et al., '71; Van Hoesen et al., '72, '75; Chavis and Pandya, '76; Rosene and Van Hoesen, '77; Jones and Powell, '78;

Accepted March 24, 1992.

Address correspondence and reprint requests to Dr. M. Mesulam, Department of Neurology, Beth Israel Hospital, 330 Brookline Ave., Boston MA 02215.

Dr. Morecraft is currently at the Department of Anatomy, University of South Dakota School of Medicine, Vermillion, SD 57069.

Yeterian and Van Hoesen, '78; Potter and Nauta, '79; Aggleton et al., '80; Baleydier and Mauguiere, '80; Barbas and Mesulam, '81; Pandya et al., '81; Porrino et al., '81; Van Hoesen, '81; Mesulam and Mufson, '82b; Porrino and Goldman-Rakic, '82; Van Hoesen, '82; Mesulam et al., '83; Amaral and Price, '84; Mesulam and Mufson, '84; Barbas and Mesulam, '85; Goldman-Rakic and Porrino, '85; Markowitsch et al., '85; Barbas and Pandya, '87; Moran et al., '87; Vogt and Pandya, '87; Yeterian and Pandya, '88; Barbas and Pandya, '89; Barbas and De Olmos, '90). In keeping with this set of connections, experimental and clinical observations indicate that this part of the brain plays a prominent role in memory, learning, emotion, motivation, higher autonomic control, olfactory-gustatory functions, and epileptogenesis (Delgado and Livingston, '48; Kaada et al., '49; Schneider et al., '64; Butter et al., '70; Iversen and Mishkin, '70; Butter and Snyder, '72; Tanabe et al., '75a,b; Thorpe et al., '83; Eslinger and Damasio, '85; Mesulam, '85; Spiers et al., '85; Damasio et al., '90; Rolls et al., '90).

Walker ('40) subdivided the orbitofrontal cortex of the monkey into five sectors which he designated areas 10, 11, 12, 13, and 14, and Bonin and Bailey ('47) subdivided the same region into areas FD, FF, and FL. More recently,

Abbreviations

a8, 9, 10, 11, 12, 13, 14, 45, 46	architectonic divisions according to Walker ('40)
AA	anterior amygdaloid area
AB	accessory basal nucleus of the amygdala
ac	anterior commissure
AM	anterior medial nucleus
amts	anterior medial temporal sulcus
AS, as	arcuate sulcus
AV	anteroventral nucleus
BL	basal lateral nucleus of the amygdala
c	claustrum
ca	caudate nucleus
CA1	CA1 sector of the hippocampus
Cdc	central densocellular nucleus
Ce	central nucleus of the amygdala
CF, cf	calcarine fissure
CG	cingulate gyrus
CGS, cgs	cingulate sulcus
Cif	central inferior nucleus
Cim	central intermediate nucleus
Cl	central lateral nucleus
Clc	central latocellular nucleus
CN	central nuclear group of the thalamus
CnMd	centromedian nucleus
Co	cortical nucleus of the amygdala
CS, cs	central sulcus
Csl	central superior lateral nucleus
Csn	central superior nucleus
cta	cortical transition area
dc	densocellular division of the medial dorsal nucleus
EC	entorhinal cortex
gp	globus pallidus
GR	gyrus rectus
hp	hippocampus
hy	hypothalamus
Iap	insula, agranular-periallocortical
ic	internal capsule
Idg	insula, dysgranular
Ig	insula, granular
InG	induseum griseum
ils	inferior limiting sulcus
IOS, ios	inferior occipital sulcus
IPS, ips	intraparietal sulcus
IS	inner cellular stratum
LD	lateral dorsal nucleus
LF, lf	lateral fissure
lgn	lateral geniculate nucleus
Li	nucleus limitans
LN	lateral nucleus of the amygdala
LOS, los	lateral orbital sulcus
LP	nucleus lateralis posterior
LS, ls	lunate sulcus
M	medial nucleus of the amygdala
mc	magnocellular division of the medial dorsal nucleus
MD	medial dorsal nucleus
MDdc	densocellular division of the medial dorsal nucleus
MDmc	magnocellular division of the medial dorsal nucleus
MDmf	multiform division of the medial dorsal nucleus
MDpc	parvicellular division of the medial dorsal nucleus
mf	multiform division of the medial dorsal nucleus
mgn	medial geniculate nucleus
MOS, mos	medial orbital sulcus
nbm	nucleus basalis of Meynert
oc	optic chiasm
OFap	orbitofrontal cortex, agranular-periallocortical
OFdg	orbitofrontal cortex, dysgranular
OFg	orbitofrontal cortex, granular
ois	orbital insular sulcus
OS	outer cellular stratum
ot	optic tract
OTS, ots	occipital temporal sulcus
Pa	paraventricular nucleus
Pac	caudal paraventricular nucleus
pc	parvicellular division of the medial dorsal nucleus
Pcn	paracentral nucleus
Pf	parafascicular nucleus
PG, PGa	architectonic divisions of cortex
PH	parahippocampal gyrus
POap	paraolfactory cortex, agranular-periallocortical
POB	paraolfactory gyrus of Broca
POC	piriform olfactory cortex
POdg	paraolfactory cortex, dysgranular
POg	paraolfactory cortex, granular
POMS	medial parieto-occipital fissure
Pr	perirhinal cortex
PS, ps	principal sulcus
Pt	parataenialis nucleus
pu	putamen
Puli	inferior division of the pulvinar nucleus
Pull	lateral division of the pulvinar nucleus
Pulm	medial division of the pulvinar nucleus
Pulo	oral division of the pulvinar nucleus
Re	reuniens nucleus
rn	red nucleus
ROS	rostral sulcus
RS, rs	rhinal sulcus
RSP	retrosplenial cortex
S	septal area
S2	supplementary sensory cortex
sls	superior limiting sulcus
sn	substantia nigra
sts, STS	superior temporal sulcus
TA, TE, TF, TH	architectonic divisions of cortex
TPap	temporal pole, agranular-periallocortical
TPdg	temporal pole, dysgranular
TPg	temporal pole, granular
TPO	architectonic division of cortex
v	ventricle
VA, Va	ventral anterior nucleus
VAmc	magnocellular division of the ventral anterior nucleus
VLc	caudal division of the ventral lateral nucleus
vldb	vertical limb of the diagonal band
VLm	medial division of the ventral lateral nucleus
VLo	oral division of the ventral lateral nucleus
VLps	postremal division of the ventral lateral nucleus
VPI	ventral posterior inferior nucleus
VPLc	caudal division of the ventral posterior lateral nucleus
VPLo	oral division of the ventral posterior lateral nucleus
VPM	ventral posterior medial nucleus
VPMpc	parvicellular division of the ventral posterior medial nucleus
vta	ventral tegmental area
X	area X

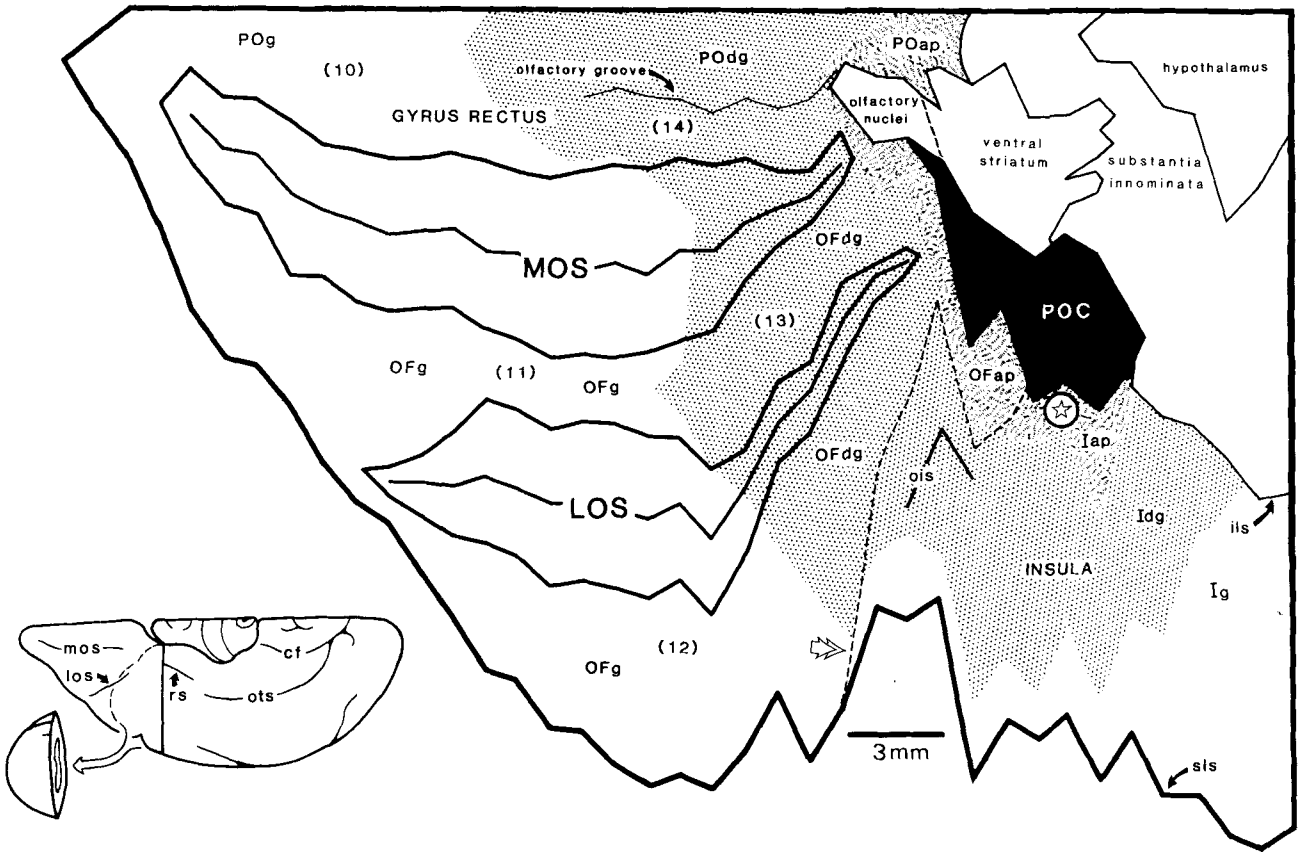

Fig. 1. Two-dimensional flattened cytoarchitectonic map of the monkey orbitofrontal cortex. The open double arrow indicates the approximate anatomical border between orbitofrontal cortex and insula. The star enclosed by a circle indicates the level at which the piriform olfactory cortex extends into the temporal pole (not shown in this illustration) along a plane that is orthogonal to the one shown in this illustration. The POC provides an allocortical root for the insular, temporopolar, and lateral orbitofrontal zones of paralimbic transition. The medial PO cortex of the gyrus rectus is continuous with two allocortical structures: the anterior olfactory nuclei that are shown in this diagram and the subcallosal extension of the induseum griseum which is not shown because of its location in the medial wall of the hemisphere. Each paralimbic zone contains agranular-periallocortical (ap), dysgranular (dg), and granular (g) sectors. Walker's terminology for the corresponding areas is shown by the numbers in parentheses. The insert at bottom left is included for purposes of orientation.

Mesulam and Mufson ('82) provided a preliminary cytoarchitectonic description of lateral orbitofrontal cortex and identified agranular, dysgranular, and granular zones, designated respectively as OFap, OFdg, and OFg.

The orbitofrontal region provides a zone of cytoarchitectonic transition between the olfactory piriform cortex and the granular association cortex of the dorsolateral frontal lobe (Rose, '27; Walker, '40; Bonin and Bailey, '47; Sanides, '69; Mesulam and Mufson, '82a). This transitional cytoarchitecture leads to the inclusion of orbitofrontal cortex within the paralimbic (mesocortical) group of cortical areas. Paralimbic areas can be divided into hippocampocentric and olfactocentric groups (Mesulam, '85). The parahippocampal, retrosplenial, cingulate, paraolfactory, and medial orbitofrontal areas belong to the hippocampocentric group of paralimbic areas where the allocortical root is the hippocampus and its induseal rudiment. The insula, temporal pole, and lateral orbitofrontal region, on the other hand, belong to the olfactocentric group in which the allocortical root is the piriform cortex.

The insular and temporopolar components of olfactocentric paralimbic areas can be subdivided architectonically into an agranular sector abutting piriform allocortex, a granular sector abutting homotypical isocortex, and an intermediate dysgranular zone interposed between the two (Mesulam and Mufson, '82a; Mesulam and Mufson, '84). Each of these cytoarchitectonic subsectors has been shown to have a differential pattern of neural connectivity such that the agranular sectors have more pronounced limbic-paralimbic connections, whereas the granular sectors have more isocortical connections (Jones and Burton, '76; Mesulam and Mufson, '82a,b; Mufson and Mesulam, '82; Mesulam and Mufson, '85; Moran et al., '87). The purpose of this study is to determine whether a similar organization exists in the cytoarchitecture and connectivity of the orbitofrontal cortex in the monkey.

MATERIALS AND METHODS

In four adult monkeys (*Macaca mulatta* and *Macaca fascicularis*) horseradish peroxidase (HRP) was injected into selected cortical regions of the orbitofrontal cortex. For cytoarchitectonic analysis, two additional monkey brains were embedded in celloidin, cut on a microtome at a thickness of 35 μm and stained with thionin.

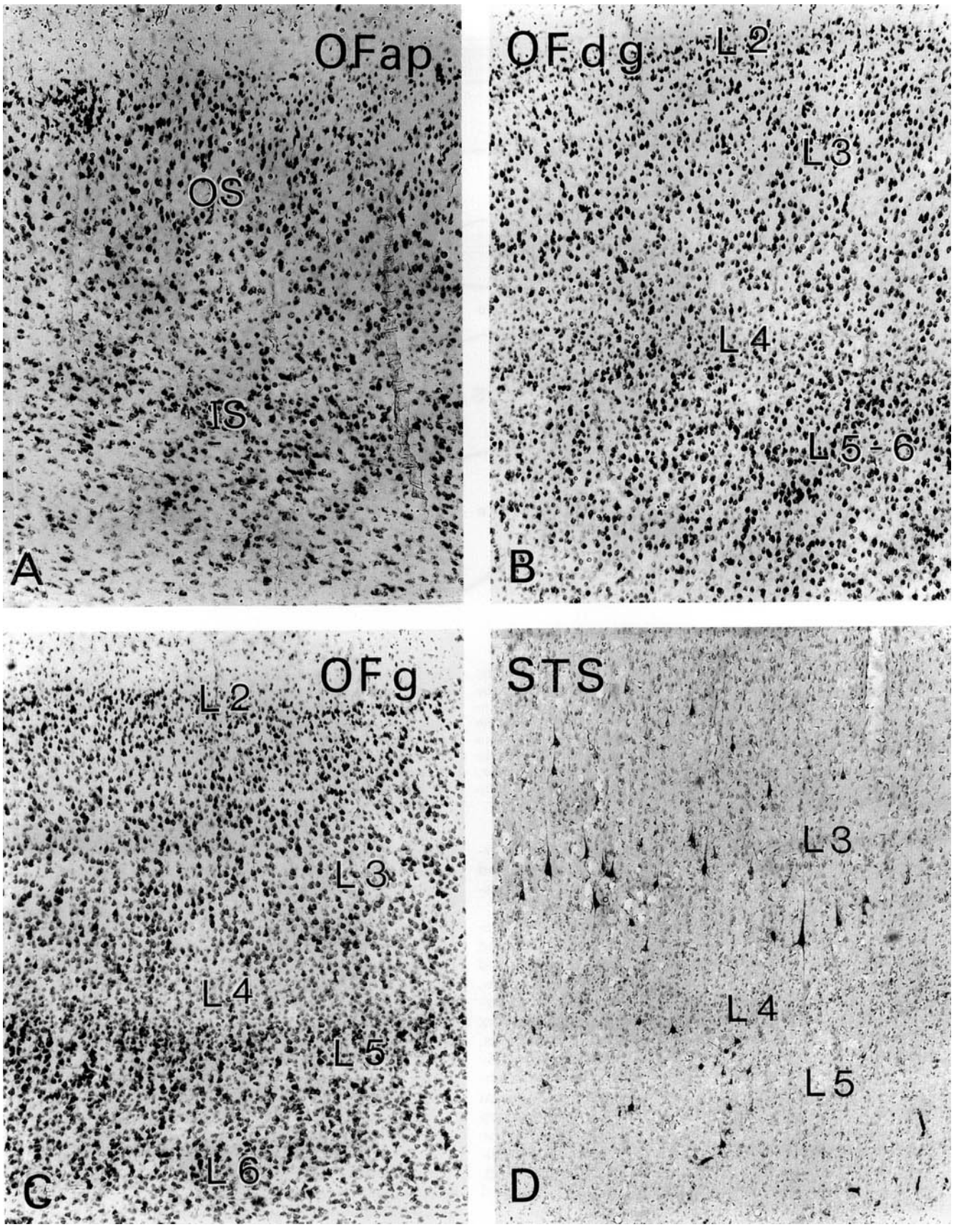

Fig. 2. Brightfield photomicrographs of the (**A**) agranular orbitofrontal cortex, displaying a simple organization consisting of an outer stratum (OS) and an inner stratum (IS) (×80), (**B**) dysgranular orbitofrontal cortex (×80), (**C**) granular orbitofrontal cortex (×80), and (**D**) HRP-labeled cells in the upper bank of the superior temporal sulcus in case 3 (×80).

Surgical technique

Each monkey was immobilized with ketamine hydrochloride, transported to the operation room, and anesthetized with intravenous sodium pentobarbital. The surgical field was shaved, cleaned, and the skull was stabilized in a head holding device. A U-shaped skin flap with its base attached to the zygomatic arch was made and the underlying galea aponeurotica and temporalis muscle were incised and reflected laterally. Following an intravenous injection of 25% mannitol (10 cc/kg), a craniotomy was performed over the prefrontal region. A dural flap was made to expose the dorsolateral surface of the frontal lobe. Cottonoid padding was inserted between the floor of the anterior cranial fossa and the opercular portion of the frontal lobe to expose the orbitofrontal cortex. The needle of a Hamilton syringe was inserted under microscopic guidance, approximately 2 mm below the cortical surface. Since our purpose was to reveal broad patterns of organization rather than the details of point-to-point connectivity, we deliberately made relatively large tracer injections. In cases 1–3, two pressure injections of 0.05 μl of a 20% solution of a 1:1 mixture of free and wheat germ agglutin (WGA)-conjugated horseradish peroxidase (HRP) were made into a selected subsector of orbitofrontal cortex. In case 4, 0.15 μl of a 30% solution was injected. Following the injection, the dura, temporalis muscle, and skin were closed using standard surgical technique.

Horseradish peroxidase histochemistry

Following a post-surgical survival period that ranged from 48 to 72 hours, each monkey was reanesthetized and perfused transcardially using fixation protocol II recommended by Rosene and Mesulam ('78). Briefly, each monkey was perfused initially with a 0.1 M phosphate-buffered saline (0.9%) solution for a period of 5 to 8 minutes. This was followed by perfusion for 30 minutes with a fixative solution containing 1% paraformaldehyde and 1.25% glutaraldehyde, and for another 30 minutes with a solution of buffered 10% sucrose. Immediately after perfusion, the brain was removed, photographed, and placed in 10% sucrose and 2% dimethyl sulfoxide (DMSO) in phosphate buffer (0.1 M phosphate, pH 7.4) for 2 days. To enhance cryoprotection, the brain was transferred to a buffered solution of 20% sucrose and 2% DMSO for 2 additional days (Rosene et al., '86). The brain was then frozen with dry ice and sectioned on a sliding microtome at a thickness of 40 μm. Three complete series of tissue sections (cut in cycles of 1 in 10) were collected and stored in sequence in a 0.1 M phosphate buffer solution. For HRP analysis, two complete series of tissue sections were processed histochemically according to a tetramethyl benzidine (TMB) procedure (Mesulam, '78, '82). Of these two series, one was counterstained with neutral red (1%) and the other was left uncounterstained. For cytoarchitectural analysis, a third series of tissue sections was stained with thionin (0.5%).

Data analysis

For cytoarchitectonic evaluation, tissue sections through the orbitofrontal cortex and rostral half of the insula were charted using a Nikon Fluophot V microscope that was electronically coupled to a Hewlett Packard X-Y plotter (HP-7045). The anatomical landmarks, white and gray matter borders, cytoarchitectonic boundaries, and the location of layer 4 (when present) were plotted in each charting. The chartings were then reconstructed, following the general guidelines of Van Essen and Maunsell ('80), to form a two-dimensional flattened cytoarchitectonic map of the monkey orbitofrontal cortex. For HRP analysis, the pertinent architectonic boundaries, injection sites, and location of retrogradely transported label in every other tissue section were charted. Our definition of the effective injec-

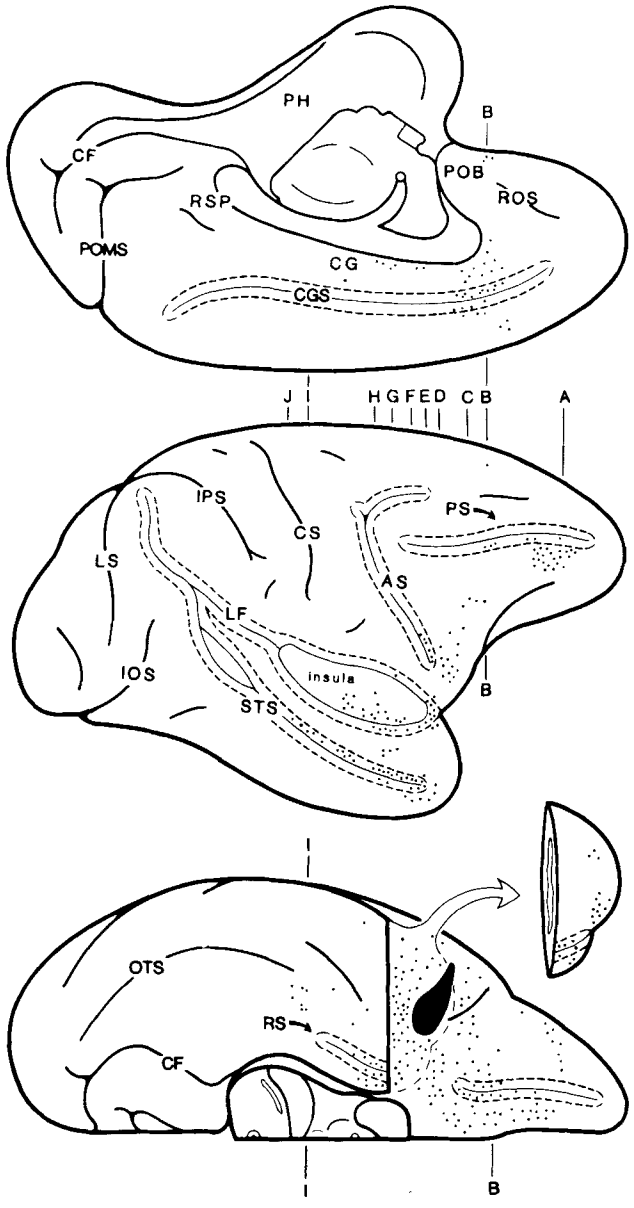

Fig. 3. Line drawing of the medial, lateral, and ventral surfaces of the cerebral hemisphere in case 1. The HRP injection site is shown in solid black and involves the dysgranular and agranular sectors of the orbitofrontal cortex. Cortical areas containing labeled neurons are indicated by black dots. The temporal pole has been removed to expose the posterior portion of the orbitofrontal cortex. The lateral fissure has been opened in the lateral view to show the insula. Note the continuity of parahippocampal (PH), retrosplenial (RSP), cingulate (CG), and paraolfactory (POB) hippocampocentric areas.

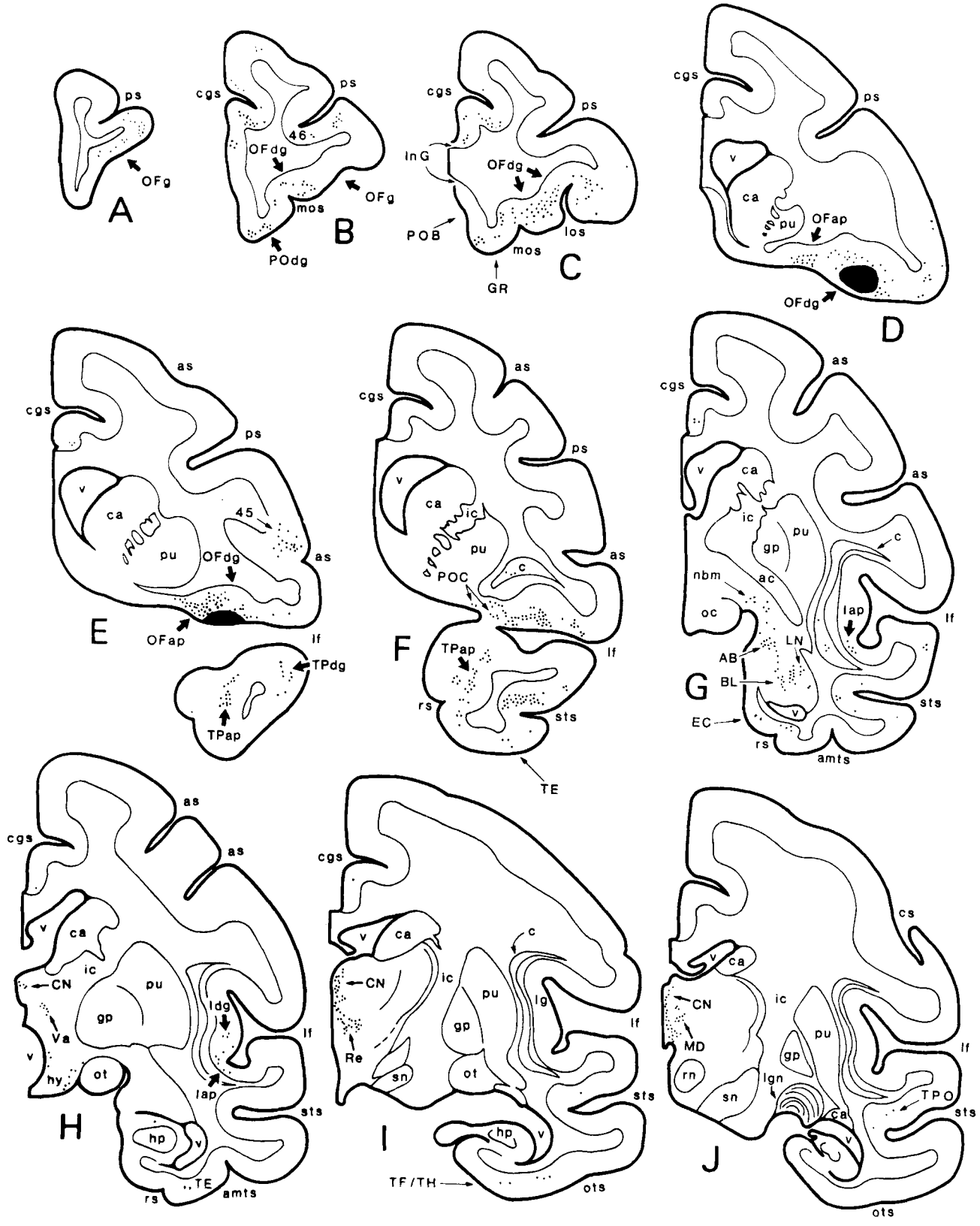

Fig. 4. Ten representative coronal sections through the brain of case 1. The HRP injection site in the orbitofrontal cortex is shown in solid black and regions containing labeled neurons are indicated by black dots. In section C, note the relationships among the induseum griseum (InG), paraolfactory gyrus of Broca (POB), and the gyrus rectus (GR).

tion site for HRP is described elsewhere (Mesulam, '82; Mufson and Mesulam, '82; Moran et al., '87).

RESULTS

The orbitofrontal cortex extends from the frontal pole rostrally to the anterior perforated substance (i.e., the ventral striatum-substantia innominata region) caudally (Fig. 1). The frontal operculum and the ventromedial margin of the cerebral hemisphere form its lateral and medial borders, respectively. The orbitofrontal cortex contains three major sulci: a shallow olfactory groove, a deep medial orbital sulcus, and a shorter lateral orbital sulcus that displays anatomical variants. There are accounts of smaller sulci which bridge the medial orbital and lateral orbital sulci to form a more complex orbitofrontal fissural pattern; however, these sulci are inconsistent in location (Mettler, '33; Connolly, '36; Walker, '40; Bonin and Bailey, '47).

The olfactory sulcus forms a shallow groove and lies hidden from direct view by the overlying olfactory tract. Lateral to the olfactory sulcus is the medial orbital sulcus. The medial orbital sulcus is the longest and most consistent of the orbital sulci and provides a boundry between the medially situated gyrus rectus and the remainder of the orbitofrontal cortex. The medial orbitofrontal sulcus and the olfactory groove provide a separation of the orbitofrontal region into medial and lateral divisions. The medial division (designated as PO cortex) is largely coextensive with the gyrus rectus. It constitutes the ventral component of Broca's paraolfactory area (POB) and can be conceptualized as a circumcallosal extension of the cingulate complex. The cortex lateral to the gyrus rectus (designated as OF cortex) is continuous with the insula and has been included within the insulo-orbito-temporopolar group of paralimbic areas (Mesulam and Mufson, '82a).

Orbitofrontal cytoarchitectonics

The overall plan of cytoarchitectonic organization reveals a concentric postero-anterior arrangement of progressively more differentiated sectors (Fig. 1). The allocortical root for the OF cortex is provided by the piriform cortex (POC), whereas the allocortical roots for the more medially placed PO cortex of the gyrus rectus can be traced to both the induseum griseum and the olfactory nuclei.

At the junction of the frontal and temporal lobes, the POC branches into three limbs. One limb extends ventrally into the temporal pole, a second limb extends laterally into the insula, and a third limb extends into the orbitofrontal surface. The orbital POC is contiguous with the agranular-periallocortex sector of lateral orbitofrontal cortex (OFap). This agranular-periallocortex sector retains a primitive and simple architecture composed of an inner and outer stratum (Fig. 2A). The inner stratum of OFap is continuous with the claustrum and the outer stratum is continuous with the POC. This sector lacks discernible groups of granule cells (Fig. 2A). At more anterior levels of the lateral orbitofrontal cortex, further architectonic differentiation occurs, analogous to that reported in the insula (Mesulam and Mufson, '82a) and temporopolar cortex (Moran et al., '87). This gradual differentiation leads to the formation of a five to six layered dysgranular cortex (OFdg) (Fig. 2B). OFdg is characterized by an emerging layer 4 which consists of a thin sheet of granule cells occasionally interrupted by the incursion of large pyramidal cells. The poorly

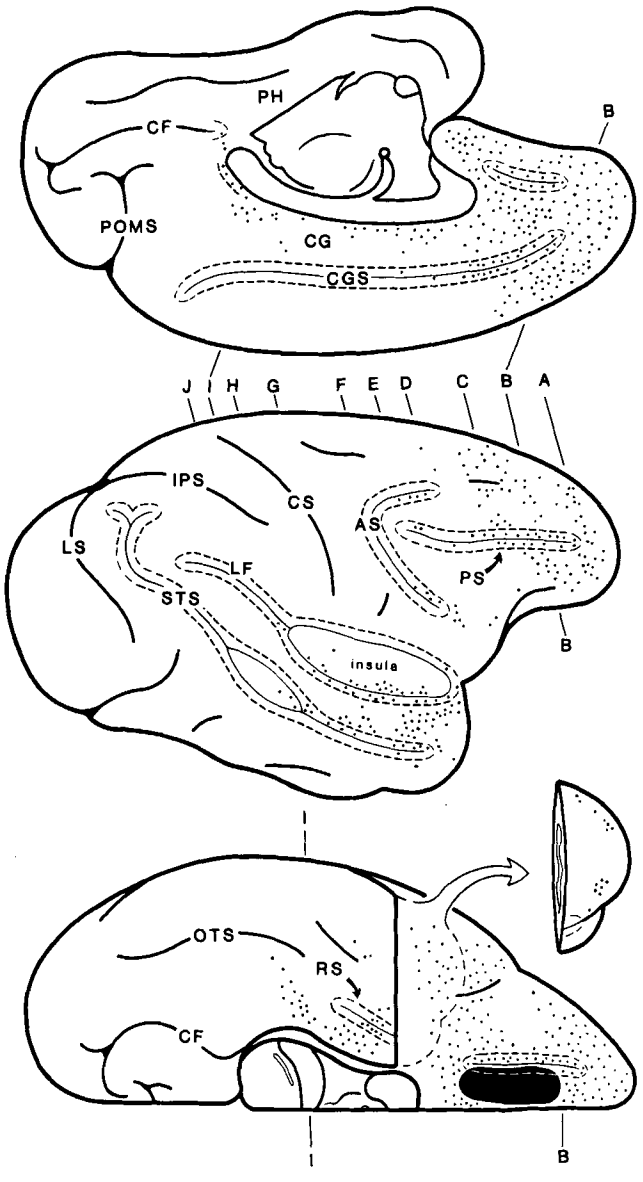

Fig. 5. Line drawing of the medial, lateral, and ventral surfaces of the cerebral hemisphere in case 2. The HRP injection site is shown in solid black and involves the granular and dysgranular sectors of the gyrus rectus. Cortical areas containing labeled neurons are indicated by black dots. The temporal pole has been removed to expose the posterior portion of the orbitofrontal cortex. The lateral fissure has been opened to show the insula.

differentiated layer 2 is difficult to distinguish from layer 3. Layers 3 and 5 lack clear evidence of sublamination, particularly at the more caudal levels of OFdg. Layer 6 is not well demarcated from layer 5 or from the underlying subcortical plate of white matter as occasional stands of neurons extend between the deeper cortical layers and the claustrum. At more anterior levels, increased granularization leads to the appearance of a six layered granular orbitofrontal cortex (OFg) (Fig. 2C). At these levels, layer 2 is somewhat better developed and layer 4 thickens. Sublamination of layer 3 is not conspicuous even though there is a greater concentration of hyperchromic pyramidal cells in

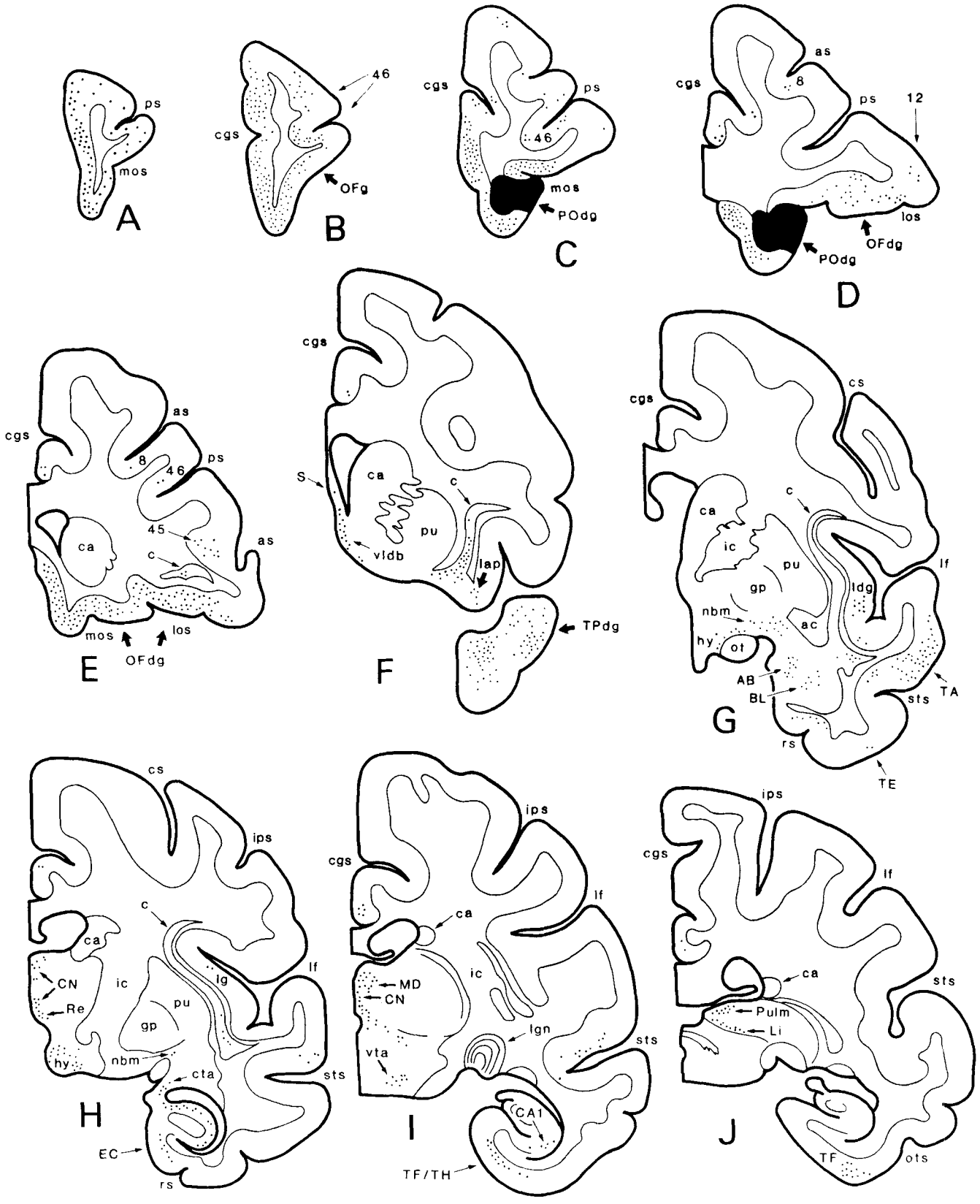

Fig. 6. Ten representative coronal sections in case 2. The HRP injection site in the orbitofrontal cortex is shown in solid black and regions containing labeled neurons are indicated by black dots.

the deeper parts of this layer. Layer 5 of OFg displays a sublamination into an external layer 5a and an internal layer 5b and is distinguished from layer 6. Additional features which characterize OFg include a sharper demarcation of layer 6 from the underlying subcortical white matter and the appearance of a more discernible radial columnar organization. Medial to the medial orbital sulcus, a parallel cytoarchitectonic organization can be identified in the PO cortex of the gyrus rectus. This region can be parcellated into a caudal agranular sector (POap), an intermediate dysgranular sector (POdg), and an anterior granular sector (POg) with cytoarchitectural features (particularly in POdg and POg) that are nearly identical to those of the analogous OF sectors.

HRP injections

Case 1. The injection site was located in the posterior portion of the orbitofrontal cortex. It was centered in the dysgranular sector of orbitofrontal cortex (OFdg), but the halo of the HRP reaction-product extended caudally to involve OFap. There was no evidence of POC or OFg involvement in the injection site. The core deposit of HRP involved layers 1 thru 4. The needle track did not enter the subcortical white matter.

Case 2. The injection site was located in the medial portion of the orbitofrontal cortex. Cytoarchitectonically, the injection site was located predominately within the dysgranular paraolfactory cortex of the gyrus rectus (POdg). The halo extended into the immediately adjacent portions of POg, OFg, and OFdg. The core deposit of HRP involved layers 1 thru 6 and approximately 1 mm of the subjacent white matter. A light HRP reaction product, continuous with the main body of the injection site, appeared over the white matter which lines the medial wall of the hemisphere.

Case 3. This injection site occupied predominately the lateral portion of the orbitofrontal cortex. The injection was situated primarily within the posterolateral part of OFg. The injectate spread into the immediately adjacent portion of OFdg. The injection site involved layers 1–6 and there was no evidence of subcortical white matter disruption.

Case 4. This injection was almost identical to that of case 2 but extended further into the medial wall of the hemisphere.

Neuronal labeling

Retrogradely labeled neurons were easily identified by the presence of a blue reaction product in the perikaryal region (Fig. 2D). The extrinsic neural projections to orbitofrontal cortex arose from a restricted set of telencephalic sources which included the dorsolateral prefrontal cortex, lateral and inferomedial temporal cortex, the cingulate-paraolfactory complex, the insula, temporal pole, hippocampus, amygdala, claustrum, basal forebrain, hypothalamus, thalamus, and brainstem (see Figs. 3–13). The results from cases 1, 2, and 3 will be described in detail. The projection pattern of case 4 was virtually identical to that in case 2.

Frontal lobe. In all cases, labeled neurons were found in areas 46, 12, and 45 of Walker ('40) (Figs. 3–8). Labeling was situated on the gyral convexity of dorsolateral prefrontal cortex as well as in the depths of the principal sulcus (Figs. 4B, 6B, 6C, 8B, 8C).Only cases 2 and 3 contained labeling within area 8 and the frontal pole. Case 1 had the most restricted pattern of labeling within the dorsolateral prefrontal cortex. Case 3 demonstrated frontal labeling also within the superior and inferior portions of the anterolateral premotor area and along the frontal operculum, extending into what appears to be the gustatory cortex (area G of Benjamin and Burton, '68 and Jones and Burton, '76) (Figs. 7, 8E).

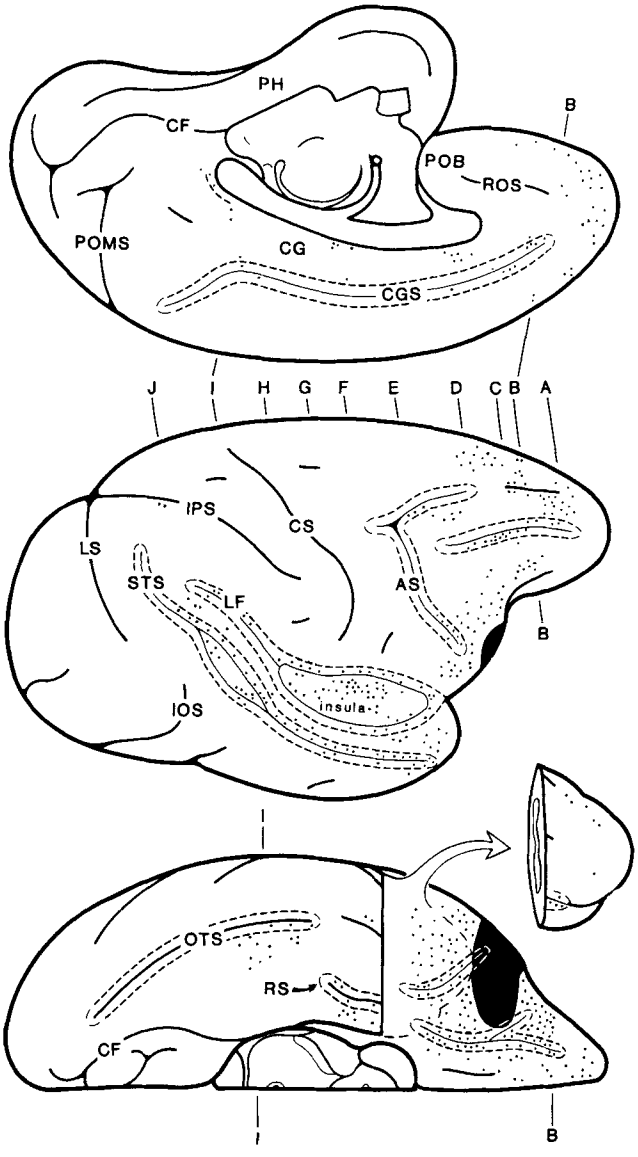

Fig. 7. Line drawing of the medial, lateral, and ventral surfaces of the cerebral hemisphere in case 3. The HRP injection site is shown in solid black and involves the granular sector of the lateral portion of the orbitofrontal cortex. Cortical areas containing labeled neurons are indicated by black dots. The temporal pole has been removed to expose the posterior portion of the orbitofrontal cortex. The lateral fissure has been opened to show the insula.

All cases showed evidence of intrinsic orbitofrontal afferents. In case 1, the density of labeled neurons was much heavier in OFdg and OFap than in OFg (Fig. 4A–E). In case 2 numerous labeled neurons were found in each of three orbitofrontal subsectors (Fig. 6A–E). Case 3 contained the most retrograde labeling in OFg and OFdg while no perikaryal labeling was detected in OFap (Figs. 7, 8). All

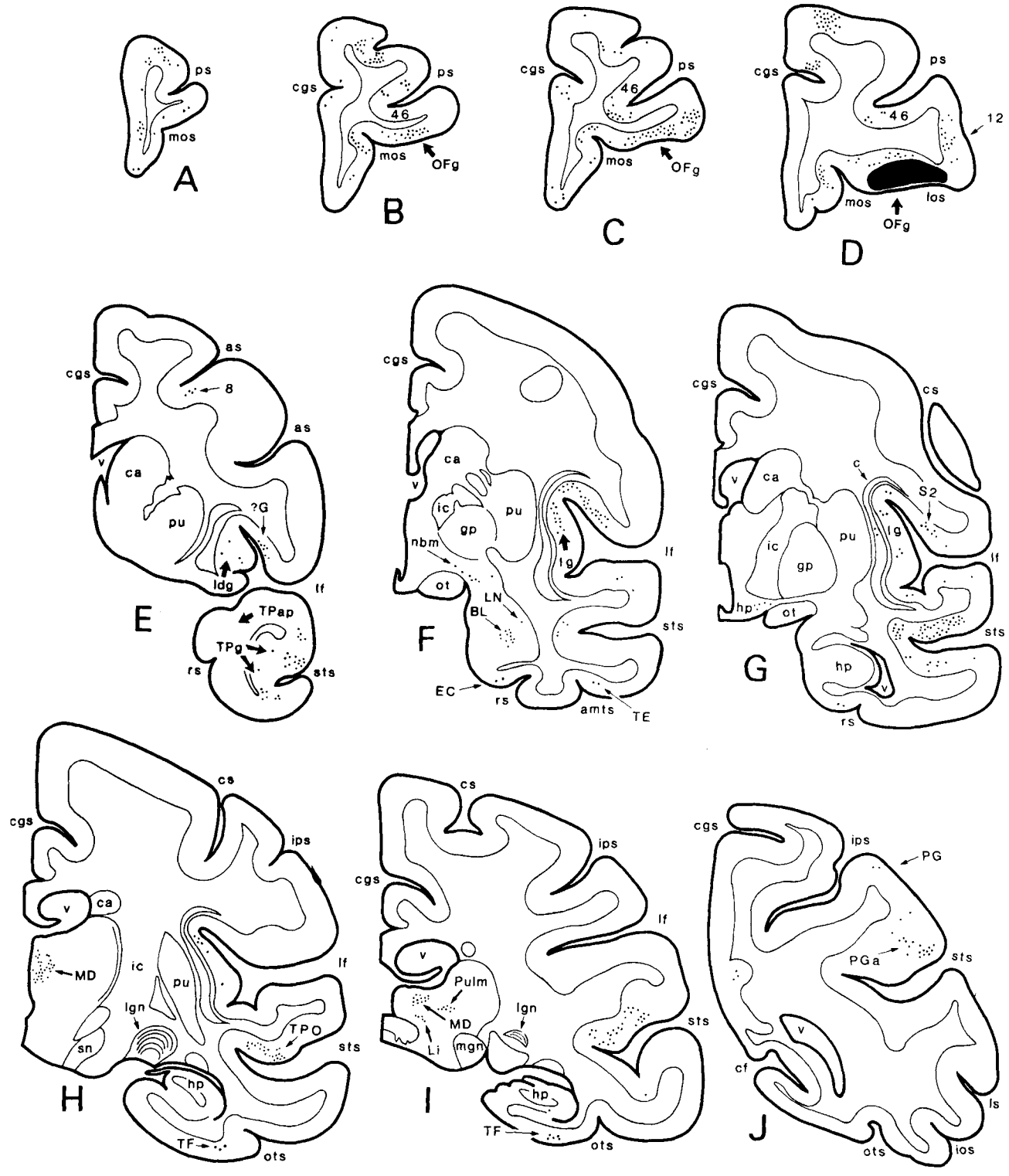

Fig. 8. Ten representative coronal sections in case 3. The HRP injection site in the orbitofrontal cortex is shown in solid black and regions containing labeled neurons are indicated by black dots.

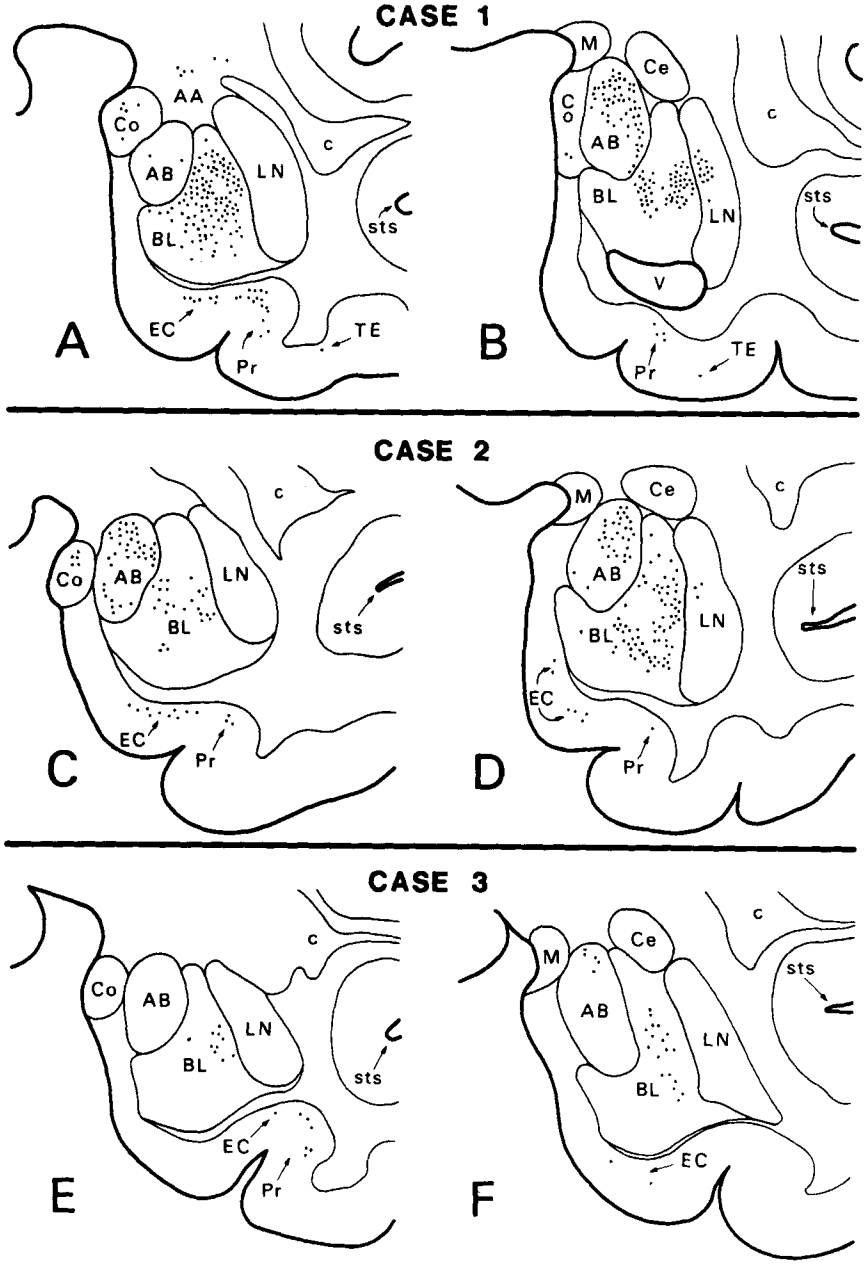

Fig. 9. Line drawings of coronal sections through the ipsilateral amygdala in cases 1, 2, and 3. The black dots demonstrate the location of HRP-labeled neurons.

three cases displayed labeling in the PO cortex of the gyrus rectus. In case 1, POdg labeling was more intense than POg labeling, whereas the converse was observed in case 3.

Lateral and inferior temporal lobe. In all cases labeled neurons were seen in the auditory association cortex of the superior temporal gyrus (area TA of Bonin and Bailey, '47) (Figs. 3, 5, 7). In all cases, numerous labeled neurons occupied the upper banks of STS [including areas TAa and TPO of Seltzer and Pandya ('78)] but only a few labeled neurons were found in the lower bank of this sulcus. In cases 1 and 2, STS labeling was concentrated within the more rostral levels of the upper bank. In case 3, STS labeling extended further caudally (Figs. 2, 8). In all cases, labeled cells were found in anteromedial TE (of Bonin and Bailey, '47) and area TF–TH (Figs. 4H–I, 6G–J, 8F–I). The TF–TH labeling was particularly prominent in case 2 (Fig. 6I).

Parietal lobe. HRP positive neurons were detected in the parietal lobe only in case 3. These neurons, few in number, were seen in area S2, the caudal-superior bank of the lateral fissure, area PGa of the superior temporal sulcus, and area PG of the inferior parietal lobule, including the ventral bank of the intraparietal sulcus (Figs. 7–8).

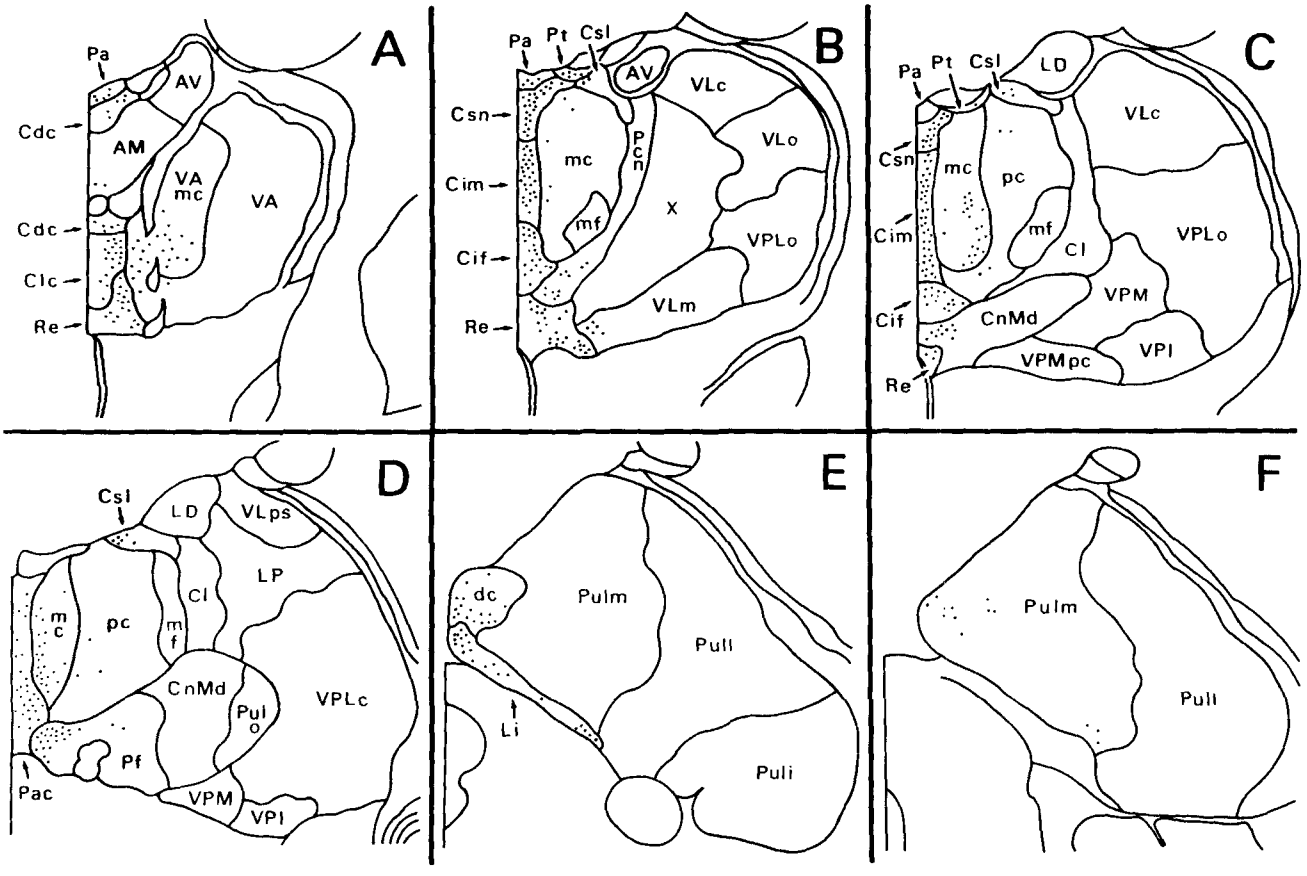

Fig. 10. Line drawings of coronal sections through the ipsilateral thalamus in case 1. The black dots show the location of HRP-labeled neurons. Note that the various subdivisions of the medial dorsal nucleus are represented as dc, mc, mf, and pc, respectively.

Cingulate cortex. In all three cases, labeled neurons were found within area 24 of the anterior cingulate cortex (Figs. 3, 5, 7). In cases 2 and 3, labeling extended posteriorly to involve area 23 and the retrosplenial cortex. Case 2 displayed the most extensive cingulate and retrosplenial labeling.

Temporal pole. In all experimental cases, labeled perikarya were identified in the temporal pole (area TG of Bonin and Bailey, '47 and TP of Mesulam and Mufson, '82a). In each case, the heaviest temporopolar labeling occurred within the cytoarchitectonic subsector analogous to that involved in the locus of the orbitofrontal injection site. For example, in cases 1 and 2, where the injection involved primarily the dysgranular and agranular sectors of cortex, the more prominent labeling was found in the dysgranular (TPdg) and agranular (TPap) sectors of temporopolar cortex (Figs. 4E, 6F). In case 3, where the injection was centered within OFg, the greatest number of labeled temporopolar neurons were located in the granular sector (TPg), less were found in TPdg, and no labeled neurons were found in TPap (Fig. 8E). Thus, individual subsectors of orbitofrontal cortex are preferentially interconnected with cytoarchitectonically analogous subsectors of temporopolar cortex.

Insula. All cases showed labeling within the insula. In cases 1 and 2, the heaviest density of labeled neurons was found in the dysgranular sector (Idg) with some extension into the agranular sector (Iap) (Figs. 4G–H, 6F–H). Case 3 demonstrated many labeled neurons in the granular sector of the insula (Ig), fewer in Idg, and no labeled cells in Iap (Fig. 8E–G). These observations suggest that individual cytoarchitectonic subsectors of orbitofrontal cortex are preferentially interconnected with analogous insular subsectors.

Entorhinal cortex, rhinal sulcus, hippocampus, and amygdala. In all cases, neuronal labeling was found in the entorhinal cortex, depths of the rhinal sulcus, hippocampus, and amygdala. In entorhinal cortex, labeling was observed mostly in the deeper layers. Entorhinal labeling was heaviest and most widespread in case 2 and least in case 3 (Figs. 3, 4G, 5, 6G–H, 7, 8F–G). Hippocampal labeling was located within the CA1 and prosubiculum sectors and was most prominent in case 2 while very few hippocampal neurons were labeled in cases 1 and 3 (Figs. 4H, 6H–I, 8I). Amygdala labeling also occurred in all three cases. The most extensive labeling was detected in cases 1 and 2 in which the injection sites involved predominately the non-isocortical (agranular-dysgranular) sectors of the orbitofrontal cortex (Figs. 4G, 6G, 8F, 9). Amygdala labeling was most intense in the basal lateral, accessory basal, and lateral nuclei. Some labeled neurons were found in the cortical nucleus and cortical transition area in cases 1 and 2

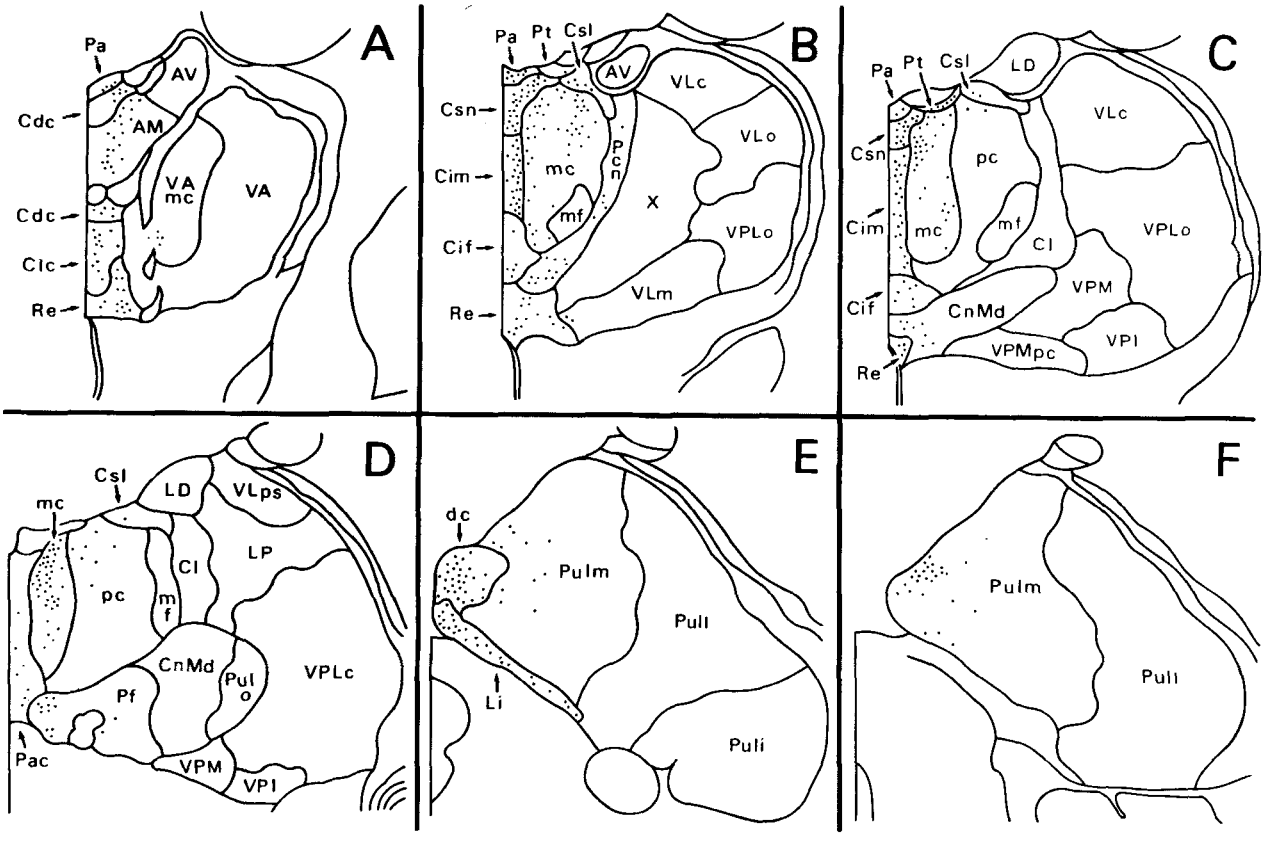

Fig. 11. Line drawings of coronal sections through the ipsilateral thalamus in case 2. The black dots show the location of HRP-labeled neurons. Note that the various subdivisions of the medial dorsal nucleus are represented as dc, mc, mf, and pc, respectively.

and a few were found in the anterior amygdaloid area in case 1 (Figs. 6H, 9).

Piriform olfactory cortex. Labeled neurons in piriform olfactory cortex (POC) were found only in cases 1 and 2 and were much more numerous in case 1 (Fig. 4F). The labeling occurred in the pyramidal cells of the orbital, insular, and temporal extensions of POC.

Hypothalamus, claustrum, septum, and nucleus basalis. HRP-filled neurons were found in the lateral, medial, and posterior hypothalamic region and the claustrum in each case (Figs. 4, 6, 8). In all cases, labeled neurons were located in the CH4-nucleus basalis complex (Mesulam et al., '83) (Figs. 4G, 6G, 8F). In case 2 a few labeled neurons were found in the vertical limb of the diagonal band and in the septal area, in regions that contain the Ch1–Ch2 cholinergic cell groups (Fig. 6F).

Thalamus. According to the nomenclature of Olszewski ('52), thalamic projections in all three cases arose from the magnocellular, parvicellular, and densocellular components of the medial dorsal nucleus; medial component of the pulvinar nucleus; magnocellular component of the ventral anterior nucleus; and medial component of the ventral lateral nucleus and the central, anteromedial, paraventricular, paratenial, paracentral, reuniens, centromedian/parafascicular, and limitans/suprageniculate nuclei (Figs. 10–12). Cases 1 and 2 received additional input from the subfascicular nucleus and case 3 from the oral component of the pulvinar nucleus and the multiform component of the medial dorsal nucleus (Figs. 12B,C). The relative distribution of labeling varied from case to case. In case 1, the vast majority of thalamic labeling was located in the midline and intralaminar nuclei (Fig. 10B–D), whereas medial dorsal and pulvinar labeling were most pronounced in case 3 (Fig. 12F). Case 2 had the most extensive labeling in the anteromedial component of the anterior thalamic tubercle (Fig. 11A).

Brainstem. Brainstem structures labeled with HRP included the ventral tegmental area, the dorsal raphe central superior nucleus, the nucleus locus coeruleus, and scattered neurons of the pontomesencephalic tegmentum. Some of these pontomesencephalic neurons were embedded in the medial longitudinal fasciculus and the superior cerebellar peduncle and probably constituted interstitial elements of the cholinergic pedunculopontine and laterodorsal tegmental nuclei.

DISCUSSION

Our findings show that the medial orbital gyrus and olfactory groove separate the orbitofrontal region into two major divisions. The medially situated gyrus rectus represents a ventral part of the paraolfactory gyrus of Broca and constitutes an anterior extension of the cingulate-retrosplenial-parahippocampal complex. Compared to the other parts

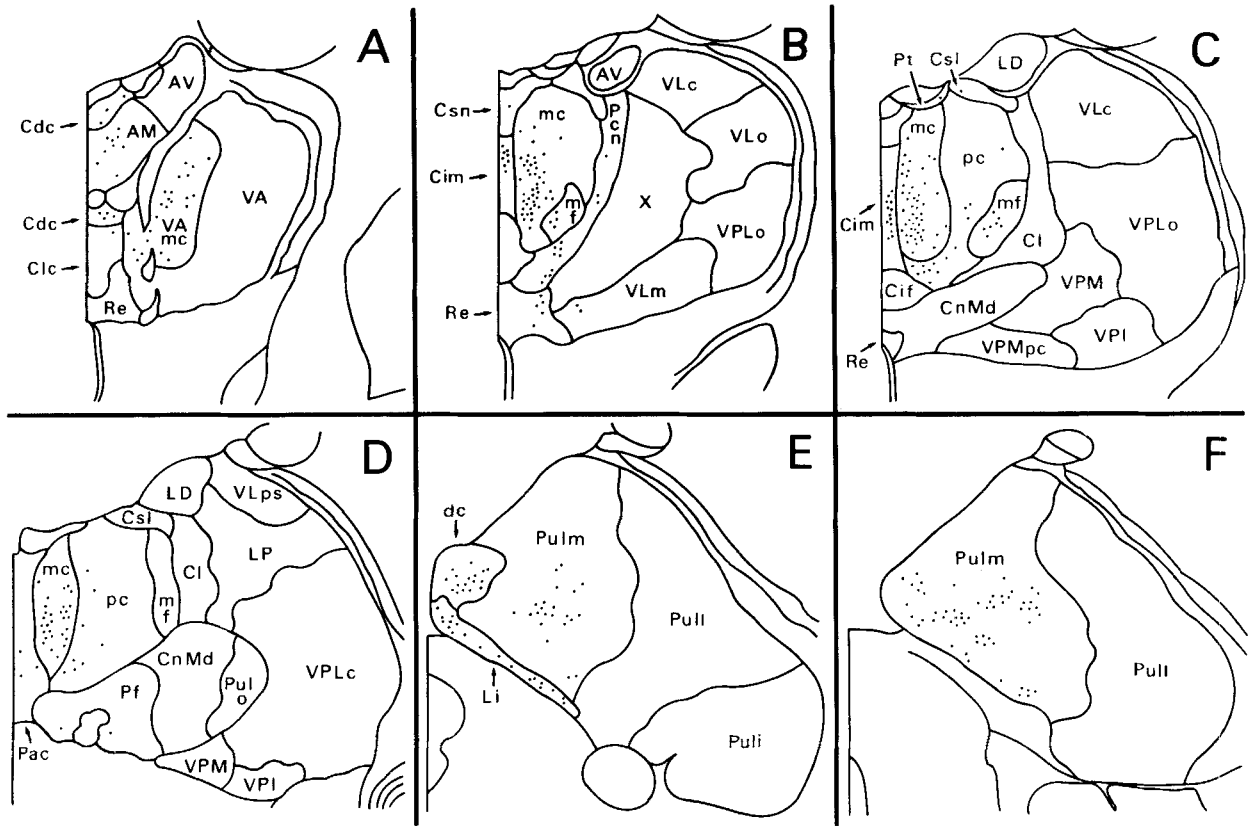

Fig. 12. Line drawings of coronal sections through the ipsilateral thalamus in case 3. The black dots show the location of HRP-labeled neurons. Note that the various subdivisions of the medial dorsal nucleus are represented as dc, mc, mf, and pc, respectively.

of the orbitofrontal region, this medial subdivision (designated PO cortex) had the most accentuated connections with the hippocampus and with additional areas known to have strong hippocampal connectivities such as the cingulate, retrosplenial and entorhinal areas, the anterior thalamic tubercle, and the septal-diagonal band nuclei (Baleydier and Mauguiere, '80; Pandya et al., '81; Van Hoesen, '82; Mesulam et al., '83; Vogt et al., '87; Vogt and Pandya, '87). These observations support our previous suggestion that this medial division of orbitofrontal cortex is closely affiliated with the *hippocampocentric* group of paralimbic areas whose major allocortical root is located in the hippocampus and its induseal rudiment (Mesulam, '85).

The cytoarchitecture and patterns of connectivity that we have observed suggest that the lateral division of orbitofrontal cortex, which we have designated OF, is more closely affiliated with the *olfactocentric* group of paralimbic areas (Mesulam and Mufson, '82a). The OF region contains three concentric rings of cortical differentiation emanating from the allocortical piriform olfactory cortex (POC) and culminating in the granular homotypical cortex of the dorsolateral prefrontal region. The most caudal and periallocortical sector of OF, OFap, is continuous with POC and has a bilaminate, agranular, and relatively undifferentiated organization. The most anterior sector, OFg, is nearly isocortical in structure and contiguous with dorsolateral prefrontal cortex. In between the two, a transitional and dysgranular sector (OFdg) can be identified. There are no definite boundaries among these three sectors. Instead, a gradual and continuous gradient of cytoarchitectonic differentiation can be identified. An analogous postero-anterior organization into POap, POdg, and POg can be identified in the medial division of orbitofrontal cortex. These observations as well as the connectivity patterns suggest that the orbitofrontal region provides a site of confluence for the olfactocentric and hippocampocentric groups of paralimbic formations.

Our observations indicate that orbitofrontal cortex derives its afferents from an anatomically restricted but functionally heterogeneous set of structures (Fig. 13). One group of afferents originates in limbic structures such as the hypothalamus, amygdala, hippocampus, olfactory piriform cortex, and midline and anterior thalamic nuclei. Additional afferents originate in paralimbic areas such as the insula, temporal pole, cingulate-retrosplenial complex, and rhinal cortices. A third group of afferents originates in the heteromodal association areas of the dorsolateral frontal cortex, the inferior parietal lobule, and the banks of the superior temporal sulcus. The relatively more downstream components of unimodal association areas in the auditory (area TAa), visual (areas TE and TF–TH), and somatosensory (area Ig) modalities also project to orbitofrontal cortex. A smaller contingent of inputs originates from the second somatosensory area (S2), gustatory cortex (G), and premotor cortex. These functionally diverse connections are in keeping with studies that have implicated orbitofrontal

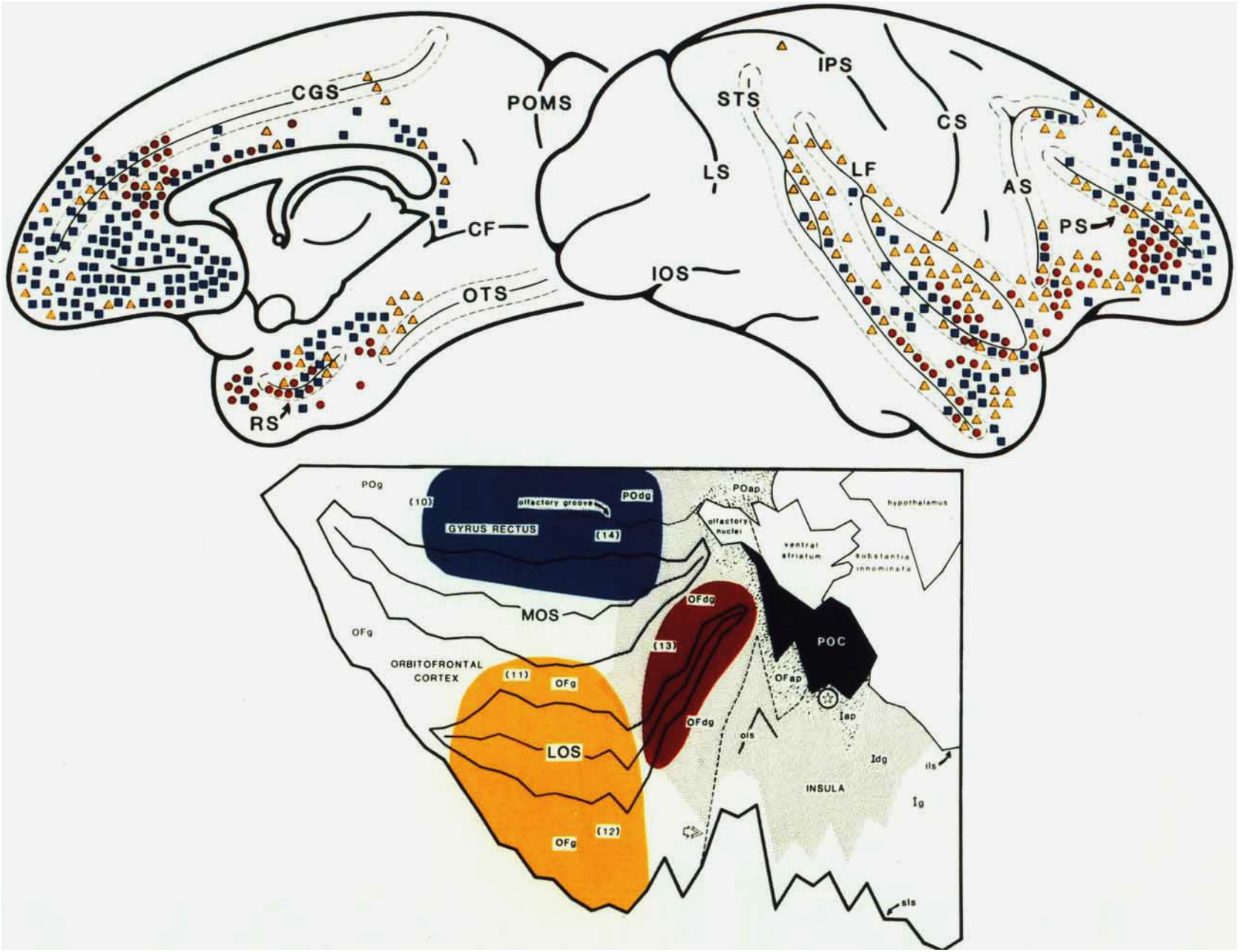

Fig. 13. Diagram summarizing the topographical distribution of afferent cortical input to the orbitofrontal cortex as determined by the three cases presented in this study. The injection site in case 1 is highlighted in red and the resultant retrograde labeling in cortex is indicated by red circles, the injection site in case 2 is shown in blue and the resultant retrograde labeling in cortex is indicated by blue squares, and the injection site in case 3 is highlighted in yellow and the resultant retrograde labeling in cortex is indicated by yellow triangles.

cortex in the modulation of emotion, memory, autonomic control, gustatory-olfactory function, and complex affiliative behaviors (Delagdo and Livingston, '48; Kaada et al., '49; Schneider et al., '64; Butter et al., '70; Iversen and Mishkin, '70; Tanabe et al., '75a,b; Thorpe et al., '83; Mesulam, '85; Rolls et al., '90).

The orbitofrontal area constitutes an important component of prefrontal cortex. Damage to the prefrontal cortex, especially in humans, gives rise to extremely complex deficits of reasoning, comportment, judgement and creativity (Harlow, 1868; Ackerly, '35; Benton, '68; Milner, '82; Eslinger and Damasio, '85; Leimkuhler and Mesulam, '85; Mesulam, '86; Damasio et al., '90; Price et al., '90). The patterns of connections that we describe indicate that the orbitofrontal component of prefrontal cortex plays a particularly prominent role in providing a site for the integration of limbic-paralimbic afferents with those coming from high-order association areas. The orbitofrontal component of prefrontal cortex may thus play a particularly crucial role in aspects of the frontal syndrome related to motivational and emotional integration. Its widespread connections with the amygdala, hippocampus, temporal pole, insula, cingulate cortex, and the parahippocampal gyrus may also explain why orbitofrontal cortex is so frequently involved in the origin and spread of temporal lobe epilepsy.

Individual sectors of lateral orbitofrontal cortex (OF) have differential patterns of connectivity that reflect their cytoarchitectonic characteristics. The non-isocortical OFap and OFdg sectors, for example, receive a heavier input from POC, the amygdaloid complex, the midline thalamic nuclei, and the non-isocortical sectors of the insula and temporal pole. These structures are all characterized by their strong limbic and paralimbic affiliations (Turner et al., '78; Rosene and Van Hoesen, '77; Mufson et al., '81; Van Hoesen, '81; Mesulam and Mufson, '82b; Mufson and Mesulam, '82; Moran et al., '87; Yeterian and Pandya, '88; Barbas and De Olmos, '90). The more differentiated and isocortical OFg component, on the other hand, receives more prominent afferents from the granular components of the insula and temporal pole, the caudal association cortex of the lateral temporal lobe, dorsolateral prefrontal cortex, inferior parietal lobule, and the medial dorsal and pulvinar nuclei of the thalamus, structures that are generally linked to high-order associative functions (Fuster, '80; Mesulam, '81; Goldman-Rakic, '87; Mesulam, '90).

An analogous pattern of differential connectivity had also been identified in other olfactocentric paralimbic areas, such as the insula and the temporal pole (Mesulam and Mufson, '82a; Mufson and Mesulam, '84; Moran et al., '87). The more non-isocortical agranular and dysgranular components of the insula (Iap, Idg) and of the temporal pole (TPap, TPdg), for example, have relatively more intense connections with limbic-paralimbic cortices, the amygdala, and limbic-midline nuclei of the thalamus, whereas the more isocortical and granular sectors of the insula (Ig) and temporal pole (TPg) have more extensive connections with association isocortex and association nuclei of the thalamus. These similarities in cytoarchitectonic organization, overall plan of connectivity and behavioral affiliations, further confirm our earlier suggestion that the orbito-insulo-temporopolar region should be collectively conceptualized as an integrated anatomical and functional system of the cerebral cortex (Mesulam and Mufson, '82a).

ACKNOWLEDGMENTS

This work was supported in part by a Javits Neuroscience Investigator Award (NS 20285 to M.-M. M) and a U.S.D. Parsons Award (to R.J.M.)

LITERATURE CITED

Ackerly, S. (1935) Instinctive, emotional and mental changes following prefrontal lobe extirpation. Am. J. Psychiatry *92:*717–729.

Aggleton, J.P., M.J. Burton, and R.E. Passingham (1980) Cortical and subcortical afferents to the amygdala of the rhesus monkey (Macaca mulatta). Brain Res. *190:*347–368.

Amaral, D.G., and J.L. Price (1984) Amygdalo-cortical projections in the monkey (*Macaca fascicularis*). J. Comp. Neurol. *230:*465–496.

Baleydier, C., and F. Mauguiere (1980) The duality of the cingulate gyrus in monkey. Brain *103:*525–554.

Barbas, H., and M.-M. Mesulam (1981) Organization of afferent input to subdivisions of area 8 in the rhesus monkey. J. Comp. Neurol. *200:*407–431.

Barbas, H., and M.-M. Mesulam (1985) Cortical afferent input to the principalis region of the rhesus monkey. Neuroscience *15:*619–637.

Barbas, H., and D.N. Pandya (1987) Architecture and frontal cortical connections of the premotor cortex (area 6) in the rhesus monkey. J. Comp. Neurol. *256:*211–228.

Barbas, H., and D.N. Pandya (1989) Architecture and intrinsic connections of the prefrontal cortex in the rhesus monkey. J. Comp. Neurol. *286:*353–375.

Barbas, H., and J. De Olmos (1990) Projections from the amygdala to basoventral and mediodorsal prefrontal regions in the rhesus monkey. J. Comp. Neurol. *300:*549–571.

Benjamin, R.M., and H. Burton (1968) Projection of taste nerve afferents to anterior opercular-insular cortex in squirrel monkey (*Saimiri sciureus*). Brain Res. *7:*221–231.

Benton A.L. (1986) Differential behavioral effects in frontal lobe disease. Neuropsychologia *6:*53–60.

Bonin, G.V., and P. Bailey (1947) The Neocortex of the Macaca Mulatta. Urbana: University of Illinois Press.

Butter, C.M., D.R. Synder, and J.A. McDonald (1970) Effects of orbital frontal lesions on aversive and aggressive behaviors in rhesus monkeys. J. Comp. Physiol. Psychol. *72:*132–144.

Butter, C.M., and D.R. Synder (1972) Alterations in aversive and aggressive behaviors following orbital frontal lesions in rhesus monkeys. Acta Neurobiol. Exp. *32:*525–565.

Chavis, D.A., and D.N. Pandya (1976) Further observations on corticofrontal connections in the rhesus monkey. Brain Res. *117:*369–386.

Connolly, C.J. (1936) The fissural pattern of the primate brain. Am. J. Phys. Anthropol. *21:*301–422.

Damasio, A.R., D. Tranel, and H. Damasio (1990) Individuals with sociopathic behavior caused by frontal damage fail to respond autonomically to social stimuli. Behav. Brain Res. *41:*81–94.

Delgado J.M.R., and R.B. Livingston (1948) Some respiratory, vascular and thermal responses to stimulation of the orbital surface of the frontal lobe. J. Neurophysiol. *11:*39–55.

Eslinger, P.J., and A.R. Damasio (1985) Severe disturbance of higher cognition after bilateral frontal lobe ablation; Patient EVR. Neurol. *35:*1731–1741.

Fuster, J.M. (1980) The Prefrontal Cortex. New York: Raven Press.

Goldman-Rakic, P.S., and L.J. Porrino (1985) The primate medial dorsal (MD) nucleus and its projection to the frontal lobe. J. Comp. Neurol. *242:*535–560.

Goldman-Rakic, P.S. (1987) Circuitry of primate prefrontal cortex and regulation of behavior by representational memory. In: V.B. Mountcastle, F. Plum, and S.R. Geiger (eds): Handbook of Physiology 5 (Part 1, Ch. 9). pp. 373–417.

Harlow, J.M. (1869) Recovery from the passage of an iron bar through the head. Mass. Med. Soc. Pub. *2:*327–346.

Iversen S.D., and M. Mishkin (1970) Perseverative interference in monkeys following selective lesions of the inferior prefrontal convexity. Exp. Brain Res. *11:*376–386.

Johnson, T.N., H.E. Rosvold, and M. Mishkin (1968) Projections from behaviorally-defined sectors of the prefrontal cortex to the basal ganglia,

septum, and diencephalon of the monkey. Exp. Neurol. *21:*20–34.

Jones, E.G., and H. Burton (1976) Areal differences in the laminar distribution of thalamic afferents in cortical fields of the insular, parietal and temporal regions of primates. J. Comp. Neurol. *168:*197–248.

Jones, E.G., and T.P.S. Powell (1970) An anatomical study of converging sensory pathways within the cerebral cortex of the monkey. Brain *93:*793–820.

Kaada B.R., K.H. Pribram, and J.A. Epstein (1949) Respiratory and vascular responses in monkeys from temporal pole, insula, orbital surface and cingulate gyrus. J. Neurophysiol. *12:*348–356.

Kuypers, H.G.J.M., M.K. Szwarcbart, M. Mishkin, and R.E. Rosvold (1965) Occipitotemporal corticocortical connections in the rhesus monkey. Exp. Neurol. *11:*245–262.

Leimkuhler, M.E., and M.-M. Mesulam (1985) Reversible go-no go deficits in a case of frontal lobe tumor. Ann. Neurol. *18:*617–619.

Levin, P.M. (1936) The efferent fibers of the frontal lobe of the monkey, *Macaca mulatta*. J. Comp. Neurol. *63:*369–419.

Markowitsch, H.J., D. Emmans, E. Irle, M. Streicher, and B. Preilowski (1985) Cortical and subcortical afferent connections of the primate's temporal pole: a study of rhesus monkeys, squirrel monkeys, and marmosets. J. Comp. Neurol. *242:*425–458.

Mesulam, M.-M. (1978) Tetramethyl benzidine for horseradish peroxidase neurohistochemistry: A non-carcinogenic blue reaction product with superior sensitivity for visualizing neural afferents and efferents. J. Histochem. Cytochem. *26:*106–117.

Mesulam, M.-M. (1981) A cortical network for directed attention and unilateral neglect. Ann. Neurol. *10:*309–325.

Mesulam, M.-M. (1982) Principles of horseradish peroxidase neurohistochemistry and their applications for tracing neural pathways-axonal transport, enzyme histochemistry and light microscopic analysis. In M.-M. Mesulam (ed): Tracing Neural Connections with Horseradish Peroxidase. New York; John Wiley and Sons, pp. 1–151.

Mesulam, M.-M. (1985) Patterns in behavioral neuroanatomy: Association areas, the limbic system, and hemispheric specialization. In M.-M. Mesulam (ed): Principles of Behavioral Neurology. Philadelphia: F.A. Davis Company, pp. 1–70.

Mesulam, M.-M. (1986) Frontal cortex and behavior. Ann. Neurol. *19:*320–325.

Mesulam, M.-M. (1990) Large-scale neurocognitive networks and distributed processing for attention, language, and memory. Ann. Neurol. *28:*597–613.

Mesulam, M.-M., and E.J. Mufson (1982a) Insula of the Old World Monkey. I. Architectonics in the insulo-orbito-temporal component of the paralimbic brain. J. Comp. Neurol. *212:*1–22.

Mesulam, M.-M., and E.J. Mufson (1982b) Insula of the old world monkey. III. Efferent cortical output and comments on function. J. Comp. Neurol. *212:*38–52.

Mesulam, M.-M., and E.J. Mufson (1984) Neural inputs into the nucleus basalis of the substantia innominata (CH4) in the rhesus monkey. Brain *107:*253–247.

Mesulam, M.-M., and E.J. Mufson (1985) The insula of Reil in man and monkey. In: A. Peters and E.G. Jones (eds): Cerebral Cortex, Vol. 4. New York: Plenum Press, pp. 179–226.

Mesulam, M.-M., E.J. Mufson, A.I. Levey, and B.H. Wainer (1983) Cholinergic innervation of cortex by the basal forebrain: Cytochemistry and cortical connections of the septal area, diagional band nuclei, nucleus basalis (substantia innominata), and hypothalamus in the rhesus monkey. J. Comp. Neurol. *214:*170–197.

Mettler, F.A. (1933) The brain of the Pithecus rhesus. Am. J. Phys. Anthropol. *17:*309–331.

Mettler, F.A. (1947a) Extracortical connections of the primate frontal cerebral cortex. I. Thalamo-cortical connections. J. Comp. Neurol. *86:*95–117.

Mettler, F.A. (1947b) Extracortical connections of the primate frontal cerebral cortex. II. Corticifugal connections. J. Comp. Neurol. *86:*119–166.

Milner, B. Some cognitive effects of frontal lobe lesions in man. Philos. Trans. R. Soc. Lond. [B] *298:*211–226.

Moran, M.A., E.J. Mufson, and M.-M. Mesulam (1987) Neural input into the temporopolar cortex of the rhesus monkey. J. Comp. Neurol. *256:*88–103.

Mufson, E.J., M.-M. Mesulam, and D.N. Pandya (1981) Insular interconnections with the amygdala in the rhesus monkey. Neurosci. *6:*1231–1248.

Mufson, E.J., and M.-M. Mesulam (1982) Insula of the old world monkey. II. Afferent cortical input and comments on the claustrum. J. Comp. Neurol. *212:*23–37.

Mufson, E.J., and M.-M. Mesulam (1984) Thalamic connections of the insula in the rhesus monkey and comments on the paralimbic connectivity of the medial pulvinar nucleus. J. Comp. Neurol. *227:*109–120.

Nauta, W.J.H. (1961) Fibre degeneration following lesions of the amygdaloid complex in the monkey. J. Anat. *95:*515–531.

Nauta, W.J.H. (1964) Some efferent connections of the prefrontal cortex in the monkey. In: Warren JM and Akert K (eds): The Frontal Granular Cortex and Behavior. New York: McGraw-Hill, pp. 397–409.

Olszewski, J. (1952) The Thalamus of the Macaca Mulatta. Basel: S. Karger.

Pandya, D.N., P. Dye, and N. Butters (1971) Efferent cortico-cortical projections of the prefrontal cortex in the rhesus monkey. Brain Res. *31:*35–46.

Pandya, D.N., and H.G.J.M. Kuypers (1969) Cortico-cortical connections in the rhesus monkey. Brain Res. *13:*13–36.

Pandya, D.N., G.W. Van Hoesen, and M.-M. Mesulam (1981) Efferent connections of the cingulate gyrus in the rhesus monkey. Exp. Brain Res. *42:*319–330.

Porrino, L.J., A.M. Crane, and P.S. Goldman-Rakic (1981) Direct and indirect pathways from the amygdala to the frontal lobe in the rhesus monkey. J. Comp. Neurol. *198:*121–136.

Porrino, L.J., and P.S. Goldman-Rakic (1982) Brainstem innervation of prefrontal and anterior cingulate in the rhesus monkey revealed by retrograde transport of HRP. J. Comp. Neurol. *205:*63–76.

Potter, H., and W.J.H. Nauta (1979) A note on the problem of olfactory associations of the orbitofrontal cortex in the monkey. Neuroscience *4:*361–367.

Price, B.H., K.R. Daffner, R.M. Stowe and M.-M. Mesulam (1990) The compartmental learning disabilities of early frontal lobe damage. Brain *113:*1383–1393.

Rolls, E.T., S. Yaxley, and Z.J. Sienkiewicz (1990) Gustatory responses of single neurons in the caudolateral orbitofrontal cortex of the macaque monkey. J. Neurophysiol. *64:*1055–1066.

Rose, M. (1927) Die sogennte Reichrinde beim Menschen und beim Affen. II. Tiel des Allocortex bei Tier und Mensch. J. Psychol. Neurol. *34:*261–401.

Rosene, D.J., and M.-M. Mesulam (1978) Fixation variables in horseradish peroxidase neurohistochemistry. I. The effects of fixation time and perfusion procedure upon activity. J. Histochem. Cytochem. *26:*28–39.

Rosene, D.L., N.J. Roy, and B.J. Davis (1986) A cryoprotection method that facilitates cutting frozen sections of whole monkey brains for histological and histochemical processing without freezing artifact. J. Histochem. Cytochem. *34:*1301–1315.

Rosene, D.L., and G.W. Van Hoesen (1977) Hippocampal efferents reach widespread areas of cerebral cortex and amygdala in the rhesus monkey. Science *198:*315–317.

Sanides, F. (1969) Comparative architectonics of the neocortex of mammals and their evolutionary interpretation. Ann. N.Y. Acad. Sci. *167:*404–423.

Schneider R.C., E.C. Crosby, and S.M. Farhat (1965) Extratemporal lesions triggering the temporal-lobe syndrome. J. Neurosurg. *22:*246–263.

Seltzer, B., and D.P. Pandya (1978) Afferent cortical connections and architectonics of the superior temporal sulcus in the rhesus monkey. Brain Res. *149:*1–24.

Spiers, P.A., D.L. Schomer, H.W. Blume, and M.-M. Mesulam (1985) Temporolimbic epilepsy and behavior. In: M.-M Mesulam (ed): Principles of Behavioral Neurology. Philadelphia: F.A. Davis Company, pp. 289–326.

Tanabe, T., M. Iino, and S.F. Takagi (1975a) Discrimination of odors in olfactory bulb, pyriform-amygdaloid areas and orbitofrontal cortex of the monkey. J. Neurophysiol. *38:*1284–1296.

Tanabe, T., H. Yarita, M. Iino, Y. Ooshima, and S.F. Takagi (1975b) An olfactory projection area in orbitofrontal cortex of the monkey. J. Neurophysiol. *38:*1269–1283.

Thorpe, S.J., E.T. Rolls, and S. Maddison (1983) The orbitofrontal cortex: Neuronal activity in the behaving monkey. Exp. Brain Res. *49:*93–115.

Turner, B.H., K.C. Gupta, and M. Mishkin (1978) The locus and cytoarchitecture of the projection areas of the olfactory bulb in Macaca mulatta. J. Comp. Neurol. *177:*381–396.

Van Essen, D.C., and J.H.R. Mausell (1980) Two-dimensional maps of the cerebral cortex. J. Comp. Neurol. *191:*255–281.

Van Hoesen, G.W. (1981) The differential distribution, diversity and sprouting of cortical projections to the amygdala in the rhesus monkey. In: Y. Ben-Ari (ed): The Amygdaloid Complex. Amsterdam: Elsevier/North-Holland Biomedical Press, pp. 77–90.

Van Hoesen, G.W. (1982) The Parahippocampal Gyrus: New observations regarding its cortical connections in the monkey. Trends Neurosci. *5*:345–350.

Van Hoesen, G.W., D.N. Pandya, and N. Butters (1972) Cortical afferents to the entorhinal cortex of the rhesus monkey. Science *175*:1471–1473.

Van Hoesen, G.W., D.N. Pandya, and N. Butters (1975) Some connections of the entorhinal (area 28) and perirhinal (area 35) cortices of the rhesus monkey. II. Frontal lobe afferents. Brain Res. *95*:25–38.

Vogt, B.A., and D.N. Pandya (1987) Cingulate cortex of the rhesus monkey. II. Cortical afferents. J. Comp. Neurol. *262*:271–289.

Vogt, B.A., D.N. Pandya, and D.L. Rosene (1987) Cingulate cortex of the rhesus monkey. I. Cytoarchitecture and thalamic afferents. J. Comp. Neurol. *262*:256–270.

Walker, A.E. (1940) A cytoarchitectural study of the prefrontal area of the macaque monkey. J. Comp. Neurol. *73*:59–86.

Yeterian, E.H., and D.N. Pandya (1988) Corticothalamic connections of paralimbic regions in the rhesus monkey. J. Comp. Neurol. *269*:130–146.

Yeterian, E.H., and G.W. Van Hoesen (1978) Cortico-striate projections in the rhesus monkey: The organization of certain cortico-caudate connections. Brain Res. *139*:43–63.